Appl. Phys. B 88, 379–384 (2007)
DOI: 10.1007/s00340-007-2742-3

Applied Physics B
Lasers and Optics

P. DOMBI[1,2,✉]
P. ANTAL[1,3]
J. FEKETE[3]
R. SZIPŐCS[3]
Z. VÁRALLYAY[4]

Chirped-pulse supercontinuum generation with a long-cavity Ti:sapphire oscillator

[1] Research Institute for Solid-State Physics and Optics, Dept. for Laser Physics, Konkoly-Thege M. út 29–33, 1121 Budapest, Hungary
[2] Institut für Photonik, Technische Universität Wien, Gusshausstr. 27/387, 1040 Wien, Austria
[3] Research Institute for Solid-State Physics and Optics, Dept. for Laser Applications, Konkoly-Thege M. út 29–33, 1121 Budapest, Hungary
[4] Furukawa Electric Institute of Technology Ltd., Késmárk u. 24–28, 1158 Budapest, Hungary

Received: 29 March 2007/Revised version: 15 June 2007
Published online: 7 August 2007 •

ABSTRACT We demonstrate chirped-pulse supercontinuum generation in a conventional fibre with a relatively narrowband, long-cavity, chirped-pulse Ti:sapphire oscillator delivering 200 nJ pulses. The inherent chirp of the outcoupled pulses were overcompensated by a 4-prism compressor to overcome damage threshold problems at the fibre entrance. The resulting fibre output spectrum corresponds to a pulse length of 7 fs in the transform-limit. The experimentally observed highly efficient spectral broadening process of negatively chirped pulses in the fibre is supported by simulation data.

PACS 42.65.Re

1 Introduction

Merging Ti:sapphire laser oscillator technology with the so-called long-cavity, chirped-pulse oscillator concept has brought significant advances in recent years [1–3]. The main objective of these development efforts was the increase of the pulse energy of femtosecond laser pulses directly available from oscillators. Thus several strong-field light-matter interaction experiments that were previously driven by oscillator-amplifier systems came within reach with relatively simple oscillators in an extremely cost-efficient manner [4]. Current state-of-the-art corresponds to pulse energies approaching the μJ frontier [3–5] and focused intensities exceeding 10^{14} W/cm^2 [4]. Moreover, further development efforts that combine this concept with cavity dumping [5] promise the possibility of the construction of μJ-level Ti:S oscillators.

Current chirped pulse oscillator technology exploits the following solutions: i) the resonator length of these lasers is increased with a so-called Herriott-cell (an imaging system with a unity ABCD matrix [6]). Since in mode-locked lasers such a cavity extension results in a decrease of the repetition rate (while the average output power usually stays the same) the energy of the outcoupled pulse can be increased. ii) However, a drastic increase that could be conceived easy by an arbitrarily huge cavity lengthening is limited by nonlinearities arising from the interaction of the focused pulses with the laser crystal. The result is pulse splitting, double pulsing and other unwanted phenomena that clamp the maximum intracavity pulse intensity in solitonically mode-locked oscillators. This drawback can be overcome by setting the net cavity dispersion either at a high negative value [1] or slightly positive [2–5] (as opposed to the slightly negative net cavity dispersion regime in which traditional soliton-like mode locking comes about). As a result, circulating mode-locked pulses in the oscillator become longer and (in the latter case) heavily chirped, and therefore they possess a lower peak intensity hindering the appearance of the above-mentioned nonlinearities. As a consequence, outcoupled pulses of a positive dispersion oscillator are also heavily chirped, but their phase modulation can be compensated for by e.g. a simple prismatic pulse compressor. iii) Since it was also noticed that an increase in cavity length results in the destabilization of the oscillator and hinders easy starting of mode-locking a saturable Bragg reflector (SBR) is introduced in the cavity which enables easy build-up and stabilization of the mode-locked operation [7, 8].

In spite of these solutions proliferating in the past 2–3 years there are some unresolved issues when it comes to the utilization of these lasers. Since their bandwidth is limited by the group delay dispersion oscillations of the chirped mirrors in the Herriott-cell and the SBR bandwidth, the shortest pulse duration available from the laser (and the subsequent linear extracavity pulse compressor) is limited to 30–60 fs [1–5]. A way to overcome this limitation is to evacuate the cavity thereby eliminating the need for chirped mirrors, however, the bandwidth in that case was also limited to 30–35 nm [4]. Even though the corresponding spectral content of these oscillators is sufficient for several novel experiments, such as material processing and nanofabrication, there are some particular spectroscopic, pump-probe and strong-field light-matter interaction experiments which call for broadening the output spectrum (and eventually pulse compression, if few-cycles pulses are necessary).

Therefore, an extracavity nonlinear element is needed for these applications in which spectral broadening of the output pulses can be carried out. Several solutions have been demonstrated in the past to achieve this for input laser pulses covering a wide range of parameter regimes. Very first demonstrations involved spectral broadening of ns pulses in single mode fibres [9] and this technique has also proven very efficient

✉ Fax: +36-1-3922215, E-mail: dombi@szfki.hu

in the femtosecond regime, too [10]. For higher peak powers bulk dielectrics are also suitable for this purpose by simply focusing the beam into them [11, 12], however, the limited interaction length (characterized by the Rayleigh range of the focused beam) and the inhomogeneous spatial profile of the spectrally broadened output beam pose a limitation to the useability of these schemes. In contrast, hollow fibre pulse compressors (filled with noble gases) found widespread use for spectral broadening of the pulses of Ti:sapphire-based oscillator–amplifier systems delivering pulses in the sub-mJ–mJ energy regime [13, 14]. However, it would be extremely difficult to downscale this concept to the intermediate pulse energy regime 100 nJ–1 μJ that is of interest to us. This is due to the fact that smaller interaction volumes are needed to achieve sufficient nonlinearity in noble gases but propagation losses scale inversely with the third power of the inner diameter of hollow fibres. More recently, microstructure fibres became known to be able to generate supercontinua from nJ-level pulses very efficiently [15, 16], however this is made possible due to their shifted zero dispersion wavelength enabled by a microstructured region around a very small (2–3 μm) core diameter. This limits their applicability in the femtosecond regime to supercontinuum generation or pulse compression of low-energy, nJ-level oscillator pulses [17–20]. Microstructure fibres are also available with large mode areas and in contrast to conventional fibres their single-mode guiding is not limited to some microns of core diameter. Using such fibres spectral broadening and subsequent pulse compression is also possible [21], however, it was demonstrated in a different parameter regime than the one of interest here. This also holds for a recent demonstration of spectral broadening of 600 nJ, 1 ps pulses in single mode fibres [22]. For the sake of completeness, tapered fibres have to be mentioned here, too, as media where efficient supercontinuum generation can be carried out, however, this technique is also limited to pulses in the nJ energy range [23, 24].

In summary, for the parameter regime of chirped pulse oscillators solid-core fibre-based solutions seem to be the most attractive, however, even optical fibres with 4–5 μm core diameters become damaged, not being able to withstand several hundreds of nJ of incoupled pulse energy. In this paper we report on a way to circumvent these problems and demonstrate an experimental solution to generate supercontinuum in a standard single-mode fibre with 200 nJ pulses of a long-cavity, chirped-pulse oscillator. We will analyze propagation phenomena of high-intensity, chirped input pulses in the fibre with simple numerical methods and demonstrate good qualitative agreement with the experimental results. The simulation code has encouraging implications for future pulse compression experiments, too.

2 Experimental setup and oscillator parameters

The setup of the oscillator that we used was very similar to previous designs. We started out from a standard Ti:sapphire laser cavity which was pumped at 9 W delivered by five lines of a multiline Ar-ion pump laser (Spectra Physics, Beamlock 2060). The crystal path length was 3.0 mm and the crystal had an absorption coefficient of $\alpha \sim 5.4\ \mathrm{cm}^{-1}$ which results in 50% absorption of the pump power. The folding mirrors have radii of curvature of 10 cm. One of the end mirrors is a 20% output coupler, the other one is a SBR which will play a role by enabling the easy start of mode-locking. There is a closely spaced fused silica Brewster prism pair that enables fine tuning of the cavity dispersion. The cavity was extended by the above-mentioned Herriott-cell system by adding an extra beam path of ~ 80 m to a round-trip by bouncing the beam several times between two 2 inch mirrors separated by 234 cm, one of which is flat, while the other has a radius of curvature of 16 m. A more detailed description and investigation of this oscillator can be found in [25].

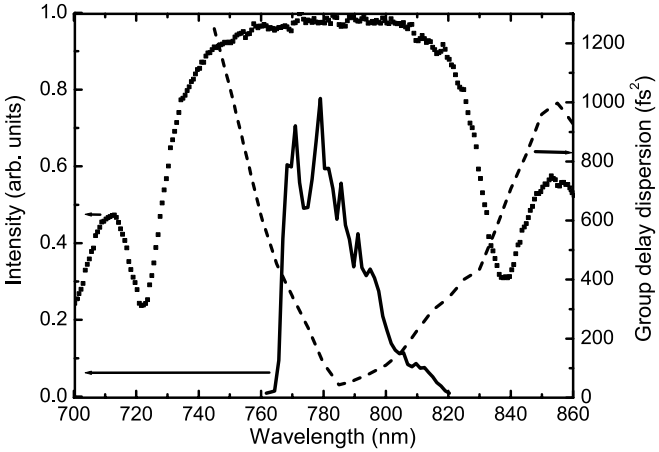

FIGURE 1 The spectrum of the chirped-pulse oscillator (*thick solid line*) together with the reflectivity of the SBR used (*squares*) and the intracavity GDD (*dashed line*) of the laser cavity as a function of wavelength

Thus the output pulses of the laser reached 200 nJ energy with a 3.6 MHz repetition rate. The oscillator spectrum was limited to a width of about 40 nm at the base. Limitations arose mainly from two factors, as depicted in Fig. 1. One was the overall spectral group delay dispersion (GDD) curve of the resonator which stays well-behaved for $\lambda > 780$ nm, where the residual third order dispersion (TOD) of the cavity stays negative and relatively small. This dispersion behaviour is mainly determined by the 2 inch Herriott-cell mirrors since the huge number of bounces magnifies any detrimental effect resulting from their spectral GDD oscillations. The measured spectrum is also in accordance with previous simulations since the effect of the non-vanishing mirror TOD can be obviously seen in the asymmetrical spectrum [26]. It is expected that by the usage of more carefully dispersion-engineered mirrors with more accurately matched dispersion oscillations one could get rid of this unwanted feature. The other bandwidth limiting factor is the reflectivity of the SBR used. Its HR region is limited to a 50 nm wide spectral range the red end of which coinciding with the red cut-off of the oscillator spectrum (Fig. 1). Using a more broadband SBR would be a solution, however, it is not trivial to manufacture such a multilayer.

The inherent heavy chirp carried by the oscillator output was then compensated by an extracavity 4-prism compressor [27] consisting of Brewster angle SF10 prisms with apex separations of 7 cm, 52 cm and 14 cm between the first and second, second and third and third and fourth prisms, respectively. Previously, a similar 4-prism compressor was used in

the chirped pulse fiber delivery system described in detail in [28]. Our present setup delivers pulses close to the transform limit determined by the width of the oscillator spectrum. This way the demonstrated laser enabled us to carry out proof-of-principle spectral broadening experiments to be described in the following section.

3 Supercontinuum generation

For reasons already mentioned in the introduction our method of choice to extend the limited spectral content of the high energy oscillator output was broadening in single-mode fibres also because preliminary experiments to broaden the spectrum in large mode area photonic crystal fibres (LMA8, Crystal Fibre) did not deliver satisfactory results, only a slight spectral broadening. The optimum solution in this case was to find a single-mode fibre for the Ti:sapphire wavelength with a maximum mode field diameter to minimize potential damage phenomena. Therefore we chose the fibre type SM750 (Fibercore) with a specified mode field diameter of 5.2 μm at 780 nm and a cut-off wavelength of 650 nm [29]. The latter parameter ensures that blue-shifted components after the expected nonlinear frequency conversion also propagate in the LP_{01} mode ensuring a utilizable output. With the help of an achromatic objective 150–160 nJ pulses after the 4-prism compressor were focussed into this fibre matching its mode-field-diameter with the focused beam waist.

Damage problems during preliminary experiments with pulses close to the transform limit (∼ 40 fs FWHM pulse length) prompted us to chirp the incoupled pulses by detuning the 4-prism compressor from the prism separation when it compensates the GDD of the oscillator output almost perfectly. Thereby we decreased the intensity at the fibre input face. For the experiments we set a net chirp of GDD $\approx -3000\,\mathrm{fs}^2$, which has an effect of a 3.5-times pulse lengthening to 140 fs, also confirmed by a commercial autocorrelator (PulseCheck). This stretching factor proved to be enough to hinder any damage occurrence, however it also reduces nonlinear frequency conversion phenomena. In spite of this, we could still observe a very broad spectrum that can be seen in Fig. 2 both on linear and on logarithmic scales together with the laser input spectrum for comparison. The transform limit of the broadened spectrum corresponds to a calculated FWHM pulse length of 7 fs which demonstrates a factor of 6–7 broadening of the initial spectrum. These findings are intriguing not just because of the substantial chirp that the broadened pulses carried but also because the simultaneous effects of negative chirp (GDD) and self phase modulation are associated with spectral narrowing [26]. This phenomenon is analyzed and explained in the next section in more detail. Our results also suggest the possibility of producing high-energy, high repetition rate pulses in the few-cycle regime, the feasibility of which is also studied.

Related to the experimental results it also has to be mentioned that we observed that the propagation in the fibre was somewhat lossy (with a maximum throughput of 35%) which manifested in both back-scattered and sideways scattered light through the cladding. The origin of this scattering process in this parameter regime is unclear and further investigations are needed to identify its roots as well as to eliminate it. Without

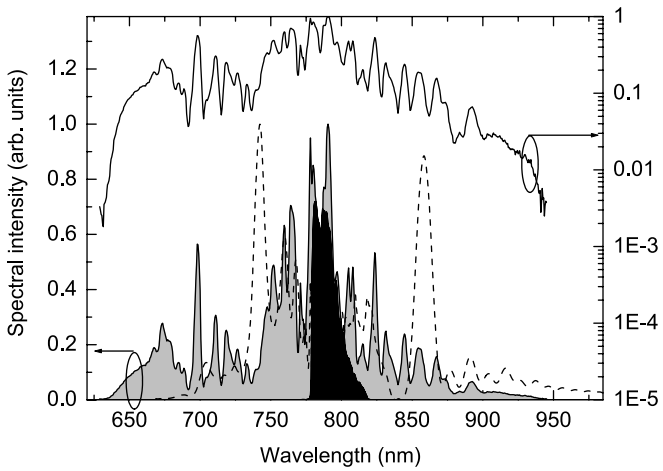

FIGURE 2 Laser oscillator spectrum (*black area*), measured supercontinuum after a single-mode fibre on linear (*gray area*) and logarithmic (*solid line*) scales. The simulated spectrum (*dashed line*) with input pulses carrying a GDD $= -3000\,\mathrm{fs}^2$ chirp is also depicted. See text for more details

a separate experimental setup to quantify this phenomenon, we can only say that based on the throughput observed and on the typical coupling efficiency of femtosecond laser beams into single mode fibres, a significant portion of the input beam (15%–35%) is back-scattered. Nevertheless, this phenomenon does not compromise our spectral broadening results and upcoming simulations since the backscattered light had a spectral width that was comparable to the fibre output spectrum. This means that most of the scattering happens after the spectral broadening process has taken place. We expect that by meticulous fibre length optimization one will be able to find a length where both reasonable throughput and large spectral width can be achieved. It is also worthwhile noting that the only work dealing with similarly high pulse energies (600 nJ) coupled into similar fibres that we are aware of, does not report this phenomenon [22]. Although those experiments were carried out with 1 ps pulses at a central wavelength of 1.5 μm and resulted in significantly less spectral broadening.

4 Numerical results and discussion

To gain insight into the experimentally observed efficient spectral broadening process resulting from the negatively chirped input pulse, we carried out numerical simulations. Light propagation in the fibre sample for these pulse lengths was modelled by using a symmetric split-step Fourier method solving a simplified form of the generalized nonlinear Schrödinger equation [30]:

$$\frac{\partial E(z,t)}{\partial z} = -\frac{\alpha}{2}E - \left(\sum_{k=2}^{N}\beta_k \frac{\mathrm{i}^{k-1}}{k!}\frac{\partial^k}{\partial t^k}\right)E + \mathrm{i}\gamma\left(|E|^2 E + \frac{\mathrm{i}}{\omega_0}\frac{\partial}{\partial t}\left(|E|^2 E\right) - T_\mathrm{R}E\frac{\partial |E|^2}{\partial t}\right), \tag{1}$$

where E is the complex envelope function, z is the coordinate on the propagation direction, t is the retarded time, α is the attenuation and β is the propagation constant. We also denoted

the respective derivatives of β as

$$\beta_k = \left(\frac{\partial^k \beta}{\partial \omega^k}\right)_{\omega=\omega_0}, \tag{2}$$

where ω is the angular frequency of light, ω_0 is the center frequency. $N = 4$ was used in our calculations. γ denotes the nonlinear coefficient in (1) given by

$$\gamma = \frac{n_2 \omega}{c A_{\text{eff}}}, \tag{3}$$

where n_2 is the nonlinear index with a value of $2.36 \times 10^{-20}\,\text{m}^2/\text{W}$ for fused silica, c is the speed of the light in vacuum and A_{eff} is the effective core area ($25\,\mu\text{m}^2$ in our case). In contrast to our previous studies with small core area PCFs [18], we included the first moment of the nonlinear Raman response, T_R in (1) that is given by

$$T_\text{R} = f_\text{R} \int_0^\infty t h_\text{R}(t)\,\text{d}t, \tag{4}$$

where f_R is the fractional Raman contribution to the nonlinear polarization chosen as 0.18 and h_R is the Raman response function approximated by an analytic form of

$$h_\text{R}(t) = \frac{\tau_1^2 + \tau_2^2}{\tau_1 \tau_2^2} \exp\left(-t/\tau_2\right) \sin\left(t/\tau_1\right), \tag{5}$$

where τ_1 and τ_2 are two adjustable parameters with the values of 12.2 fs and 32 fs, respectively.

In order to describe the pulses obtained from the laser oscillator properly we defined the spectral shape of the envelope either by the measured spectral shape or, for more general studies, by a higher-order super-Gaussian function

$$\tilde{E}(z=0,\omega) = \sqrt{\tilde{P}_0} \exp\left(-\frac{1}{2}\frac{\omega^{2m}}{\Delta\omega^{2m}}\right), \tag{6}$$

where $\Delta\omega$ is the spectral width of the pulse, m is the Gaussian order set to be 3. The tilde sign above the quantities denotes quantities in the Fourier-space. We were prompted to choose this analytic function for the spectral shape by the fact that we obtained very similar results when we used the measured asymmetric oscillator spectrum for the simulations. The chosen super-Gaussian shape, however, describes a more general case and it approximates the observed spectral properties of other similar oscillators. In order to obtain the necessary input temporal shape a carefully selected phase function with a non-vanishing GDD value was added to the spectrum and transformed to the temporal space.

A Taylor-polynomial up to the third order described the fibre dispersion ($D = -104.352\,\text{ps}/(\text{nm km})$, $S = 0.3984\,\text{ps}/(\text{nm}^2\,\text{km})$ at the reference wavelength of 840 nm). Since the pulse length at the fibre input was ~ 140 fs in our experiments, we set the chirp of the input pulses the following way: $\text{GDD} = -3000\,\text{fs}^2$, $\text{TOD} = 0\,\text{fs}^3$. We used these parameters for propagation simulations together with intensity data calculated from the mode field diameter of the fibre and the pulse energy. With these circumstances and using the measured spectral shape for the numerical input good qualitative agreement could be achieved with the measured data apart from a slight red-shift of the simulated spectrum at the fibre output (Fig. 2) which can be attributed to the simplified nonlinear Schrödinger equation (1) that we used. In spite of this slight difference, we found that both the measured and the simulated spectra (Fig. 2) correspond to a transform-limited FWHM pulse length of ~ 7 fs, thereby providing good agreement on the extent of the spectral broadening process.

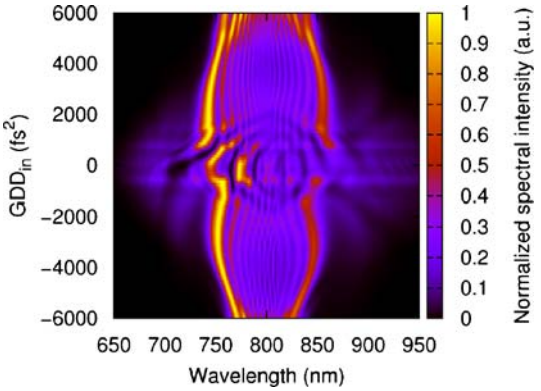

FIGURE 3 Computed spectral intensity of the fibre-based supercontinuum in false colour representation for different linear chirp values of the input pulse. For parameters see text

To investigate phenomena that take place along the fibre we carried out more general modelling with the super-Gaussian input spectrum. Here we noticed that the initially negatively chirped pulses propagate in the fibre with an unchanged/slightly narrowing spectrum and an almost constant temporal shape up to a length of 0.3 mm. This corresponds to twice the computed nonlinear length of 0.147 mm. After this point the spectrum continuously broadens while the temporal length of the pulse that starts to acquire a quasi-rectangular shape and remains unchanged and about 400 fs long. After a certain point there is not any significant spectral broadening any more and the pulse becomes even longer, reaching 800 fs after a propagation length of 50 mm.

It is also insightful to take a closer look at the influence of the chirp carried by the pulses at the fibre input. Therefore, simulations were carried out with the same parameters as above for a fibre length of 10 mm for the $\text{GDD} = -6000\,\text{fs}^2$–$6000\,\text{fs}^2$ input chirp range while keeping $\text{TOD} = 0\,\text{fs}^3$. Whereas for the close-to-transform-limited case a much more efficient spectral broadening process is observed (Fig. 3), as expected (even though experimentally this would mean damaging the fibre), for positively chirped pulses a similar spectral width can be reached comparable to the case of negatively chirped pulses. From the symmetry of the false colour plot to the $\text{GDD} = 0\,\text{fs}^2$ line (Fig. 3) we can conclude that it is primarily the length of the input pulse (or, equivalently, the absolute value of the linear input chirp) that determines the extent of spectral broadening. Beyond mere spectral broadening, however, in some experiments one may intend to compress the high energy broadband output from such a fibre. In the following it will be revealed that in this case negative input GDD is favoured.

In order to examine the compressibility of the fibre output we carried out further simulations. Obviously, there is a trade-off between the spectral width and the amount of nearly linear

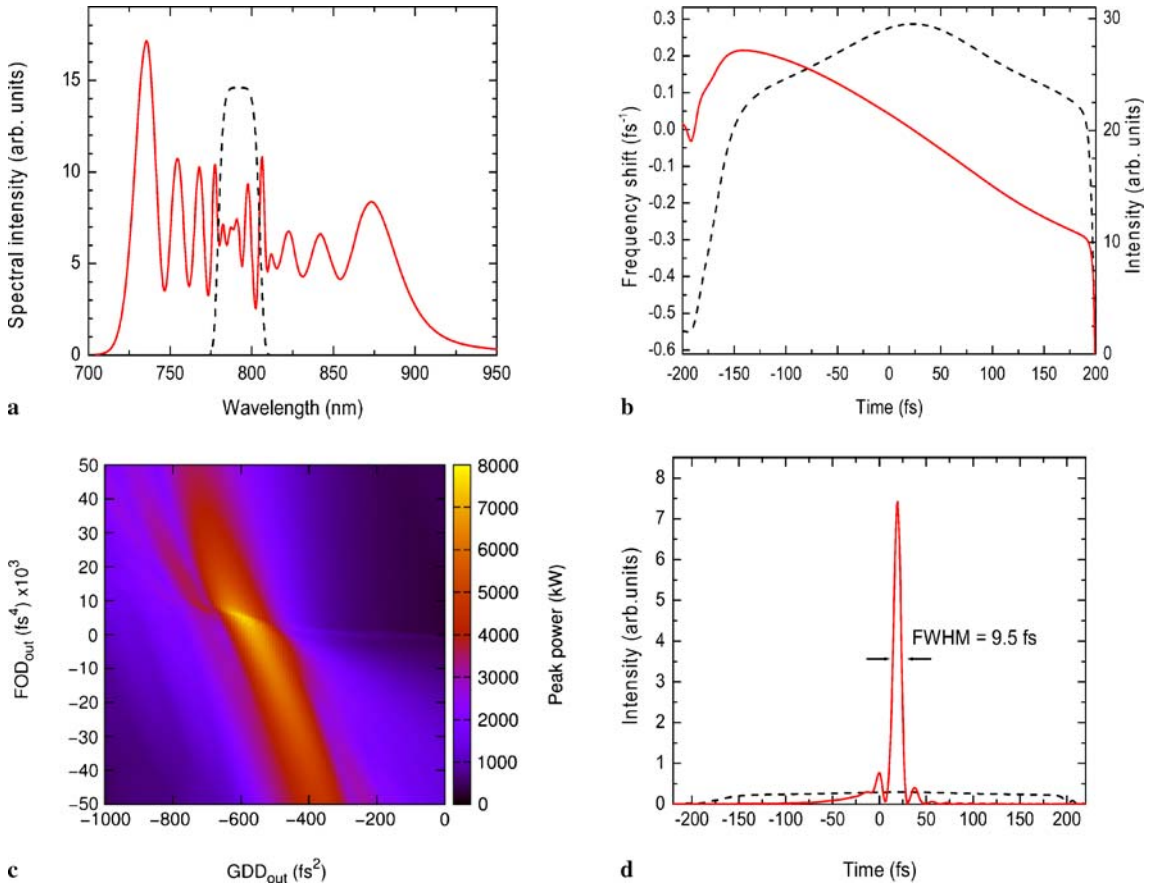

FIGURE 4 (**a**) Computed spectral broadening after a propagation length of 10 mm (*solid curve*). The input spectrum is also shown (*dashed curve*). For input parameters see text. (**b**) Computed intensity vs. time function of a spectrally broadened pulse after 10 mm propagation in a single mode fibre (*dashed curve*). The actual frequency shift relative to the carrier frequency is also shown (*solid curve*). (**c**) Relative peak intensity values of the continuum generated in a single mode fibre with a length of 10 mm as a function of GDD and FOD compensation. (**d**) Computed temporal shape of the uncompensated (*dashed curve*) and the compressed (*solid curve*) continuum pulse exiting a single mode fibre with a length of 10 mm

positive chirp of the output continuum to be compensated when choosing the fibre length: the shorter the fibre the narrower is the self-phase modulated spectrum. However, shorter fibres result in a lower negative GDD needed to compensate the chirp of the pulse. Therefore, we performed a simulation in which we chose a fibre length of $L = 10$ mm, but used practically the same data we used for the simulation shown in Fig. 2. As we will show, this fibre length results in a chirp that can be easily compensated in practice, but still provides efficient spectral broadening for sub-10-fs pulses, as shown in Fig. 4a. In Fig. 4b we show the computed temporal shape and the frequency shift relative to the central frequency of the pulse, the latter corresponding to 792 nm. One can observe that the chirp is nearly linear with some superimposed higher-order dispersion. In order to determine the optimum parameters for compression, we calculated a peak intensity map shown in Fig. 4c. We found that the pulse has not any third-order chirp, hence we can set TOD $= 0$ fs^3 for optimum compression. However, besides the negative GDD the fourth-order dispersion (FOD) should be compensated as well, as shown in Fig. 4c. Thus the optimum dispersion compensation values were found to be GDD $= -580$ fs^2, TOD $= 0$ fs^3, FOD $= 5000$ fs^4. Using these values, we calculated the temporal shape of the continuum after such an ideal compressor (see Fig. 4d). The compressed pulse exhibits a FWHM temporal width of 9.5 fs, which is well suited for different applications listed in the introduction. According to further numerical checks the generated spectral shape and phase remain robust to 1%–2% pulse energy fluctuation in contrast to supercontinua generated in the anomalous dispersion regime [17, 31]. This also confirms the expected robustness of the proposed compression method. Experiments to optimize the fibre length for pulse compression will be subject of a future study.

5 Summary and outlook

In this paper we have experimentally demonstrated that efficient spectral broadening of chirped femtosecond pulses with hundreds of nJ is possible in single-mode fibres. Thereby we suggested a way to circumnavigate damage threshold problems at the fibre entrance and showed a way to extend the spectral content of high energy Ti:sapphire oscillator pulses in a simple setup. Our results are directly exploitable in spectroscopic measurements where broadband, energetic, high repetition rate pulses are desired. Furthermore, our numerical results point out that in such an experimental scheme pulse compression factors of 4–6 are feasible by accurate fibre length optimization, thereby proposing a way to generate sub-microjoule few-cycle pulses with unprece-

dented repetition rates. These findings can help in developing chirped-pulse Ti:sapphire oscillator technology further, by furnishing it for novel spectroscopic, time-resolved, micromachining and biomedical applications in the future.

ACKNOWLEDGEMENTS We acknowledge the advice and help of S. Naumov and A. Apolonskiy with setting up the oscillator and fruitful discussions with G. Farkas. The generous loan of optical test equipment by the Research Institute for Experimental Medicine, R&D Ultrafast Lasers Ltd., and the financial support of the Hungarian Scientific Research Fund (OTKA, grants T49296 and F60256) are also gratefully acknowledged. This work was also supported by the Max Planck Institute for Quantum Optics in the framework of a "Kooperationsvertrag".

REFERENCES

1 S.H. Cho, F.X. Kärtner, U. Morgner, E.P. Ippen, J.G. Fujimoto, J.E. Cunningham, W.H. Knox, Opt. Lett. **26**, 560 (2001)
2 A. Fernandez, T. Fuji, A. Poppe, A. Fürbach, F. Krausz, A. Apolonski, Opt. Lett. **29**, 1366 (2004)
3 S. Naumov, A. Fernandez, R. Graf, P. Dombi, F. Krausz, A. Apolonski, New J. Phys. **7**, 216 (2005)
4 S. Dewald, T. Lang, C.D. Schröter, R. Moshammer, J. Ullrich, M. Siegel, U. Morgner, Opt. Lett. **31**, 2072 (2006)
5 X.B. Zhou, H. Kapteyn, M. Murnane, Opt. Express **14**, 9750 (2006)
6 D. Herriott, H. Kogelnik, R. Kompfner, Appl. Opt. **3**, 523 (1964)
7 U. Keller, G.W. 't Hooft, W.H. Knox, J.E. Cunningham, Opt. Lett. **16**, 1022 (1991)
8 U. Keller, K.J. Weingarten, F.X. Kärtner, D. Kopf, B. Braun, I.D. Jung, R. Fluck, C. Honninger, N. Matuschek, J. aus der Au, IEEE J. Sel. Top. Quantum Electron. **2**, 435 (1996)
9 C. Lin, R.H. Stolen, Appl. Phys. Lett. **28**, 216 (1976)
10 V.S. Yakovlev, P. Dombi, G. Tempea, C. Lemell, J. Burgdörfer, T. Udem, A. Apolonski, Appl. Phys. B **76**, 329 (2003)
11 C. Rolland, P.B. Corkum, J. Opt. Soc. Am. B **5**, 641 (1988)
12 E. Mével, O. Tcherbakoff, F. Salin, E. Constant, J. Opt. Soc. Am. B **20**, 105 (2003)
13 M. Nisoli, S. De Silvestri, O. Svelto, Appl. Phys. Lett. **68**, 2793 (1996)
14 M. Nisoli, S. DeSilvestri, O. Svelto, R. Szipőcs, K. Ferencz, Ch. Spielmann, S. Sartania, F. Krausz, Opt. Lett. **22**, 522 (1997)
15 W.J. Wadsworth, A. Ortigosa-Blanch, J.C. Knight, T.A. Birks, T.P.M. Man, P.St.J. Russell, J. Opt. Soc. Am. B **19**, 2148 (2002)
16 J.M. Dudley, G. Genty, S. Coen, Rev. Mod. Phys. **78**, 1135 (2006)
17 S. Lakó, J. Seres, P. Apai, J. Balázs, R.S. Windeler, R. Szipőcs, Appl. Phys. B **76**, 267 (2003)
18 Z. Várallyay, J. Fekete, Á. Bányász, R. Szipőcs, Appl. Phys. B **86**, 567 (2007)
19 K. Yamane, Z. Zhang, K. Oka, R. Morita, M. Yamashita, Opt. Lett. **28**, 2258 (2004)
20 B. Schenkel, R. Paschotta, U. Keller, J. Opt. Soc. Am. B **22**, 687 (2005)
21 T. Südmeyer, F. Brunner, E. Innerhofer, R. Paschotta, K. Furusawa, J.C. Baggett, T.M. Monro, D.J. Richardson, U. Keller, Opt. Lett. **28**, 1951 (2003)
22 J.W. Walewski, J.A. Filipa, C.L. Hagen, S.T. Sanders, Appl. Phys. B **83**, 75 (2006)
23 T.A. Birks, W.J. Wadsworth, P.St.J. Russell, Opt. Lett. **25**, 1415 (2000)
24 D.A. Akimov, A.A. Ivanov, M.V. Alfimov, S.N. Bagayev, T.A. Birks, W.J. Wadsworth, P.St.J. Russell, A.B. Fedotov, V.S. Pivtsov, A.A. Podshivalov, A.M. Zheltikov, Appl. Phys. B **74**, 307 (2002)
25 P. Dombi, P. Antal, Laser Phys. Lett. **4**, 534 (2007)
26 V.L. Kalashnikov, E. Podivilov, A. Chernykh, S. Naumov, A. Fernandez, R. Graf, A. Apolonski, New J. Phys. **7**, 217 (2005)
27 B. Proctor, F. Wise, Opt. Lett. **17**, 1295 (1992)
28 B. Rózsa, G. Katona, E.S. Vizi, Z. Várallyay, A. Sághy, L. Valenta, P. Maák, J. Fekete, Á. Bányász, R. Szipőcs, Appl. Opt. **46**, 1860 (2007)
29 www.fibercore.com
30 G.P. Agrawal, *Nonlinear Fiber Optics* (Academic, San Diego, CA, 2007), Chapt. 2
31 A.L. Gaeta, Opt. Lett. **27**, 924 (2002)